IEEE Transactions on Nuclear Science, Vol. NS-28, No. 3, June 1981

HEAVY ION INJECTION FROM TANDEMS INTO AN ISOCHRONOUS CYCLOTRON

M.J. LeVine and C. Chasman*
Brookhaven National Laboratory, Upton, New York 11973 USA

Summary

A design has been realized for the injection of heavy ion beams generated by the BNL 3-stage tandem facility into a proposed isochronous cyclotron. The tandem beams are bunched into ±1° R.F. phase (≤0.5 nsec) in two stages. The beam is then injected into the cyclotron through a valley, past a hill, and into the next valley on to a stripper foil. Only a single steerer is required to make trajectory corrections for the different beams. Two achromats are used to regulate the tandem potential and to provide phase control. A final section of the injection optics provides matching of transverse phase space to the acceptance of the cyclotron. The calculations use realistic tandem emittances and magnetic fields for the cyclotron based on measurements with a model magnet.

The proposed BNL cyclotron

Brookhaven National Laboratory proposes to build a cyclotron addition to the existing 3-stage tandem Van de Graaff facility. This addition will provide a large variety of heavy ion beams will range up to 150 MeV/amu for light heavy ions and up to 16 MeV/amu for uranium, with energy resolution of 4×10^{-4} ($\Delta E/E$). The proposed cyclotron is a 4-hill, room temperature, isochronous machine, with radius R=240 cm. Beams from the present tandem facility will be bunched and injected into the cyclotron, where they will be stripped and accelerated. The layout of the proposed facility is shown in Fig. 1. The subject of this paper is the bunching and preparation of tandem beams for injection. Other aspects of the cyclotron design are discussed elsewhere.[1]

Energy limitations imposed by injection

For A>40, injection considerations play a major role in determining the maximum energy which can be accelerated for each ion species. Several strongly interdependent considerations are involved: The combined efficiency of the tandem and cyclotron strippers was required to exceed 1%. Charge state yields are calculated following Betz.[2] The voltages of the two tandems have been limited to -8.5 MV and +13.5 MV. Finally, all of the beams must originate from a single point outside the cyclotron with a single steerer making minor corrections (±1°) to the injection trajectory to match it to the first equilibrium orbit.

Characteristics of some typical beams are given in Table 1. The stripper moves radially over a total distance of 27 cm and 5° azimuthally (see Fig. 2).

Bunching

Bunching of the beam must to produce beam pulses corresponding to ±1° of RF phase (δt = 0.3-0.5 nsec). This will result in a pulse length contribution to energy resolution of 1.5×10^{-4} for the extracted beam, while yielding a negligible contribution to radial smearing of orbits at the extraction radius.

Bunching occurs in two stages. Primary bunching will take place after the beam leaves the tandem source and will produce pulses 1-2 nsec in length at the output of the tandem. Further bunching takes place at the rebuncher, midway between the tandem and the cyclotron, producing bunches of the required length at the stripper in the cyclotron.

A separated function two-harmonic buncher will be employed as primary buncher. These bunchers have been described in detail by Milner[3] and have been shown to bunch as much as 70 percent of the DC beam.

In order to minimize the growth of longitudinal phase space due to energy straggling at the tandem stripper, the time focus will be located at the stripper. Most of the time spread at the rebuncher occurs due to the energy straggling arising from the gas stripper in the tandem terminal. This energy straggling has been estimated based on the measurements of Schmidt-Böcking and Hornung[4].

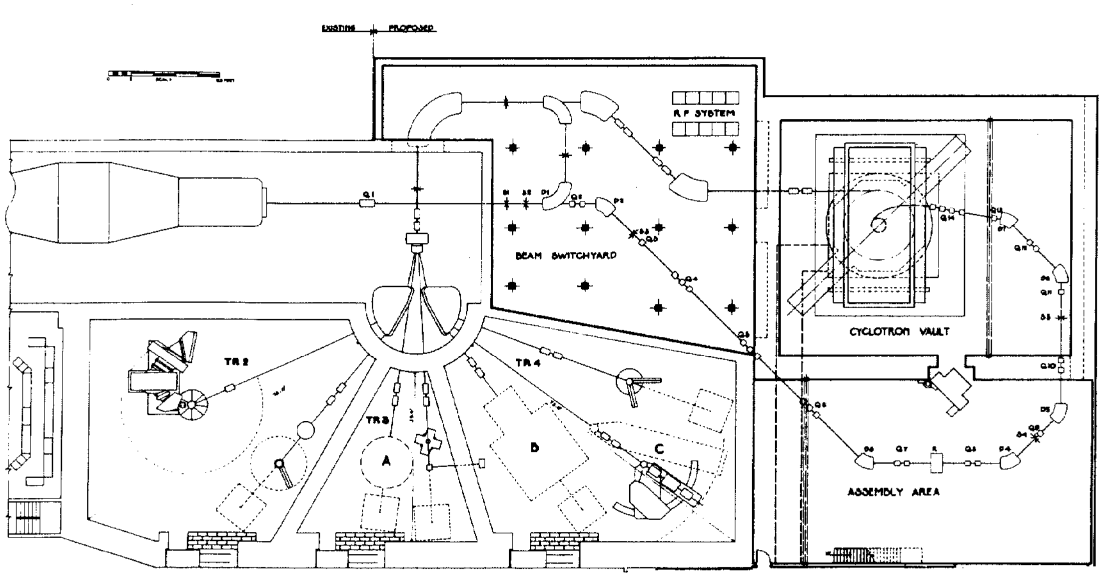

Fig. 1. Layout of the proposed facility. Injection system elements are D (dipole), Q (quadrupole), S (slit), and R (rebuncher).

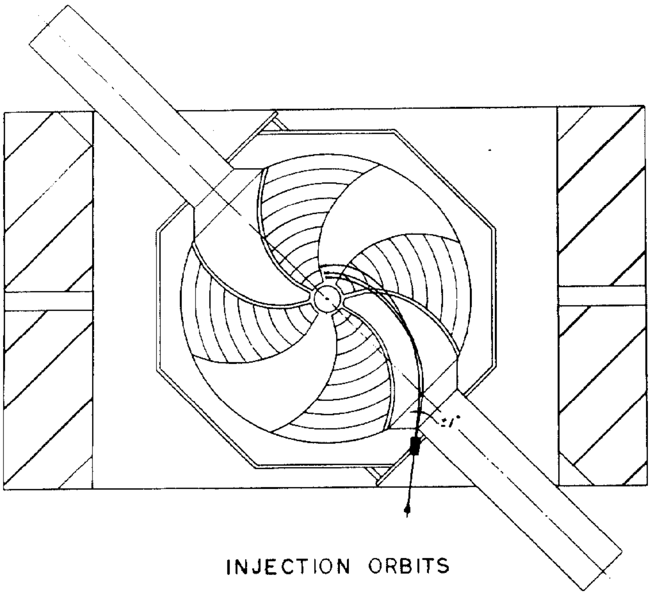

Fig. 2. Injection trajectories are illustrated for oxygen beams (8 and 150 MeV/amu) as well as for a 16 MeV/amu uranium beam.

The rebuncher is a tuned cavity with impressed potential rates of up to 32 kV/nsec (Table 1). The energy modulation introduced by the rebuncher is typically 3×10^{-3} of the beam energy. Other contributions to the beam energy spread must be kept to ~0.3 of the rebuncher modulation; energy stability of the tandems of about 9×10^{-4} is therefore required.

Not only must the bunch length be kept to the tolerances noted above, but the bunch centroid is subject to equally stringent requirements with respect to the RF phase. Relatively minor potential redistributions in the tandem column can result in centroid shifts of tens of nanoseconds.[5] It is therefore essential to detect and correct such shifts in order to guarantee that the beam produced by the cyclotron is of uniformly high quality.

In order to achieve this, magnetic phase analysis is employed. Because a properly phased beam enters the rebuncher at a zero-crossing of the impressed potential, a phase error results in an energy shift in the mean energy of the beam following the rebuncher. These errors are sensed by the slits of the momentum analysis system following the rebuncher; resulting error signals can be used to modulate the pre-acceleration potential or to change the phase of the primary buncher. Details of the phase analysis system are presented below.

Injection optics (K=350)

The purpose of the injection optics is to match the output phase space of the tandems to the cyclotron acceptance at the stripper. The emittance of the tandem varies slightly (see Table 1) from one beam to another, but the focussing properties of the cyclotron field crossed by the injected beam vary wildly for different beams. Thus the injection optics must compensate for this variation, presenting a spot on the cyclotron stripper whose dimensions are approximately the same (2 mm x 3 mm) for all beams.

Determination of the focussing properties of the cyclotron for the injected beams was made: Realistic fields were generated by scaling from model magnet measurements[1], including contributions from the 27 trim coils. Trajectories were calculated for a central ray and for 10 rays displaced from the central ray in x,θ,y,ϕ, using a version of the code GOBLIN[6] suitably modified for this purpose. The 10 rays chosen allowed the determination of the effects on longitudinal and transverse phase space and permitted the monitoring of second-order effects.

The most complicated aspect, however, arises from longitudinal phase space (E-t) considerations. The design goal here is to present a beam on the stripper foil whose time spread corresponds to no more than $\pm 1^{\circ}$ of RF phase: all path length differences must not exceed 1.6mm for the most stringent case, ^{238}U at 2.5MeV/amu. Since path length differences in the bending magnets required for energy and phase analysis can amount to 2 cm, these dispersive elements must be carefully compensated by other bends.

Finally, at two places in the injection system, the rebuncher and the cyclotron stripper, the transverse and longitudinal phase space must be decoupled. Otherwise, adjustments to the rebuncher would degrade the focussing, and vice versa.

The injection optics consists of four distinct sections (Fig. 1): energy analysis (S2-Q7), phase analysis (Q8-Q10), dispersion matching (Q11-Q13), and matching lens (Q14). The first two sections are independent of the beam injected. The third section compensates for path length differences within the cyclotron and the matching lens compensates for the focussing properties of the cyclotron. The injection system begins at the tandem object slits, S2.

Use of a bending magnet always results in a coupling of the longitudinal (E-t) and transverse (x-θ) planes of the beam phase space, i.e., $R_{16},R_{26},R_{51},R_{52} \neq 0$, where R is the transport matrix and the indices 1,...,6 stand for $x,\theta,y,\phi,\ell,\delta$ (TRANSPORT notation[10]). The relation between the path length elements $R_{51} = (\ell|x)$ and $R_{52} = (\ell|\theta)$ and the dispersion elements $R_{16} = (x|\delta)$ and $R_{26} = (\theta|\delta)$ is given by Refs. 11,12. In order to uncouple the longitudinal and transverse planes, i.e., to obtain $R_{51} = R_{52} = 0$, it is necessary to have $R_{16} = R_{26} = 0$ (achromatic condition).

A convenient way to achieve this is by exploiting the cancellations inherent in mirror symmetric systems.[12] If a second bending magnet follows the first, symmetric about a focus in the horizontal plane between them, one achieves $R_{16} = 0$. If, in addition, a quadrupole lens is placed in the symmetry plane, $R_{26} = 0$ can be achieved as well. This is the basis for the achromatic systems which are used extensively in the injection system. The symmetry required extends only over the region where dispersion is nonzero: the lenses preceding the first and following the second bending element are not part of the achromat and are used to control transverse phase space.[13]

The energy analysis achromat consists of two 45° bends. The first bend (D2) provides energy analysis slits (S3) for tandem energy control and removal of unwanted charge states. At this point D/M = 2.75 cm/%. With a spot size of 1.5 mm at the object slit (S2), $p/\Delta p$ = 1835 at S3, which corresponds to an energy control capability[14] of one part in 12000 using logarithmic current amplifiers. This is adequate for our needs (E/E 9×10^{-4}). Between the two 45° bends is a 20m long 3-triplet array (Q4-Q6) which reproduces the beam from slit S3 with magnification $M_x = -1$, thus allowing the subsequent asymmetric bend (D3) to cancel matrix element $(x|\delta)$ arising from the preceding bending section. The quadrupole singlet Q3 allows $(\theta|\delta)$ to be set to zero: the elements of importance here, $(\ell|x)$ and $(\ell|\theta)$ are both zero. Hence the longitudinal and transverse components of phase space are decoupled at the rebuncher, where a focus exists in both horizontal and vertical directions as well.

In order to retain adequate control of the y envelope of the beam further downstream, the y angular magnification has been kept small at the cost of giving up exact achromaticity. In particular, the matrix element $(\ell|x) \sim 0.54$. The corresponding pulse length, 0.6mm, is still well within design tolerance.

The 20m long 3-triplet array which forms the intermediate section of the energy analysis achromat, is a symmetric array of symmetric triplets, so that four independent parameters are available to guarantee diagonal transport matrices in both the x-θ and y-ø planes. The symmetry of the array guarantees that $|M_x| = |M_y| = 1$ (unity magnification) is a possible solution.

The phase achromat provides momentum analysis capabilities at slit S4 which will control the phase of the bunched beam with respect to the cyclotron RF. Since D4 and D5 bend in the same direction, the intermediate inverting section found in the energy achromat is not required here.

The dispersion matching section consists of two symmetric 40^o bends, D6 and D7. The variation in dispersive elements due to the cyclotron is compensated here. An intermediate horizontal focus exists near the symmetry plane. If the focus were at the symmetry plane, $(\ell|\theta) = 0$. Adjusting the x-focus displacement from the symmetry plane as well as adjusting the quadrupole pair Q12 allows adjustment of the elements $(\ell|x)$ and $(\ell|\theta)$ over the necessary range without affecting the transverse focussing substantially.

The final section consisting of four quadrupoles (Q14) performs two tasks. Not only are erect ellipses produced in x-θ and y-ø at the stripper, but the matrix element $(\ell|x)$ is cancelled by this section, since it becomes increasingly difficult to control further upstream.

Because the various beam transport sections presented here will be tuned separately, it would be advantageous to have each of the sections completely independent of the other; i.e., the submatrices for x-θ and y-ø should be diagonal for each section. This has been approximately achieved for each section. Although the off-diagonal elements R_{43} and R_{21} are not zero, they are sufficiently small (~1) so that buildup of angular spread is unimportant, and coupling between sections is negligible.

The computer code TRANSPORT[10] was used extensively in carrying out the design calculations.

References

* Work supported by the U.S. Department of Energy under Contract No. DE-AC02-76HU0016.
1) C.E. Thorn, C. Chasman, and A.J. Baltz, contribution to this conference; and A.J. Baltz, C. Chasman, and C.E. Thorn, contribution to this conference.
2) H.D. Betz, Rev. Mod. Phys. 44, 465 (1972).
3) W.T. Milner, IEEE Trans. Nucl. Sci. NS26, 1445 (1979).
4) H. Schmidt-Böcking and H. Hornung, Z. für Phys. A 286, 253 (1978).
5) J.H. Ormrod, Chalk River National Laboratories, private communication.
6) GOBLIN, computer code provided by E. Heighway, CRNL.
7) W.R. Brandt, R. Laubert, M. Mourins, and A.Z. Schwarzschild, Phys. Rev. Lett. 30, 358 (1973).
8) G. Doucas, H. R. Hyder, and A. B. Knox, Nucl. Instrum. Methods 124, 11 (1975).
9) C.K. Cline, T. E. Pierce, K. H. Purser, and M. Blann, Phys. Rev. 180,450 (1969).
10) K.L. Brown, B.K. Kear, and S.K. Howry, Stanford Linear Accelerator Report SLAC-91.
11) K.L. Brown, Stanford Linear Accelerator Report SLAC-75 (1967), pp. 78-79.
12) J.C. Herrera and E.E. Bliamptis, Rev. Sci. Instrum. 37, 183 (1966).
13) G. Hinderer and K.H. Maier, IEEE Trans. Nucl. Sci. NS22, 1722 (1975).
14) W.G. Davies and A.R. Rutledge, IEEE Trans. Nucl. Sci. NS26, 2086 (1979).

Table 1. Some characteristics of eight beams for which detailed injection calculations have been carried out.

Ion	E/A MeV/amu	E_{inj} (MeV)	K MeV·amu	Q_i	r_{inj} (cm)	Q_f	B(240cm) (kG)	RF (MHz)	Harmonic Number	Energy Straggling (keV)[1]	Rebuncher Energy Modulation (keV/nsec)	Rebuncher Amplitude (kV)	Emittance Before Foil[2,3] (mm-mrad)	Mean Ang. Scatt. in Foil[3] (mrad)
^{16}O	150	35.0	140	2	32.0	8	15.3	20.20	2	10.3	64.4	127	2.62π	0.85
^{16}O	8.0	8.0	32	2	58.6	5	5.4	15.53	6	7.3	7.0	18	4.49π	1.3
^{60}Ni	100	88.0	210	5	31.0	21	17.6	17.08	2	30.1	113.3	106	1.40π	0.8
^{60}Ni	5.0	18.0	68	4	57.9	10	8.0	20.52	10	11.9	10.5	10	3.18π	1.15
^{127}I	51	143.5	225	9	35.8	31	17.8	18.97	3	34.8	160.5	75	0.94π	0.54
^{127}I	3.5	18.0	135	4	49.0	11	13.0	17.19	10	12.3	7.2	8	2.76π	0.86
^{238}U	16	135.0	320	10	44.7	33	17.4	14.55	4	29.2	107.1	58	0.94π	0.63
^{238}U	2.5	20.0	300	4	43.8	13	17.4	14.54	10	12.9	6.2	8	2.39π	0.82

[1]Ref. 4 [2]Refs. 7, 8 [3]Ref. 9